

Study of Acyl Group Migration by Femtosecond Transient Absorption Spectroscopy and Computational Chemistry

Elena A. Pritchina,^{†,‡,§} Nina P. Gritsan,^{*,‡,§} Gotard T. Burdzinski,^{†,||} and Matthew S. Platz[†]

Department of Chemistry, The Ohio State University, 100 West 18th Avenue, Columbus, Ohio 43210, Institute of Chemical Kinetics and Combustion, Siberian Branch of Russian Academy of Sciences, 3 Institutskaya Street, 630090 Novosibirsk, Russia, Novosibirsk State University, 2 Pirogova Street, 630090 Novosibirsk, Russia, and the Quantum Electronics Laboratory, Faculty of Physics, Adam Mickiewicz University, 85 Umultowska, Poznan 61-614, Poland

Received: May 15, 2007; In Final Form: July 17, 2007

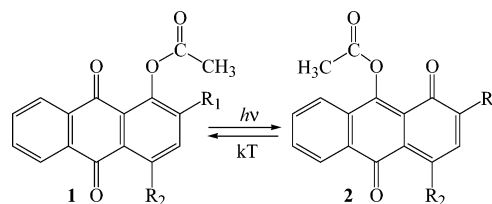
The primary photophysical and photochemical processes in the photochemistry of 1-acetoxy-2-methoxyanthraquinone (**1a**) were studied using femtosecond transient absorption spectroscopy. Excitation of **1a** at 270 nm results in the population of a set of highly excited singlet states. Internal conversion to the lowest singlet $n\pi^*$ excited state, followed by an intramolecular vibrational energy redistribution (IVR) process, proceeds with a time constant of 150 ± 90 fs. The $^1n\pi^*$ excited state undergoes very fast intersystem crossing (ISC, 11 ± 1 ps) to form the lowest triplet $\pi\pi^*$ excited state which contains excess vibrational energy. The vibrational cooling occurs somewhat faster (4 ± 1 ps) than ISC. The primary photochemical process, migration of acetoxy group, proceeds on the triplet potential energy surface with a time constant of 220 ± 30 ps. The transient absorption spectra of the lowest singlet and triplet excited states of **1a**, as well as the triplet excited state of the product, 9-acetoxy-2-methoxy-1,10-anthraquinone (**2a**), were detected. The assignments of the transient absorption spectra were supported by time-dependent DFT calculations of the UV–vis spectra of the proposed intermediates. All of the stationary points for acyl group migration on the triplet and ground state singlet potential energy surfaces were localized, and the influence of the acyl group substitution on the rate constants of the photochemical and thermal processes was analyzed.

Introduction

Acyl group migration reactions are common in chemistry and biochemistry. For instance, acyl transfer is the fundamental bond-forming reaction in the biosynthesis of proteins. Another example of acyl migration is the very well studied Fries rearrangement,¹ which also has a photochemical counterpart—the photo-Fries rearrangement.² The radical mechanism of the photo-Fries rearrangement is well established^{2c–f} and manifests itself in the formation of a multitude of photoproducts. To improve the selectivity, the photo-Fries rearrangement was recently performed in water-soluble, confined assemblies.³ It is also known that this rearrangement occurs mainly through the excited singlet state.^{2d–f}

Another type of photochemical acyl migration has been observed for a series of 1-acetoxy-9,10-anthraquinone derivatives.^{4a} It was found that this process is thermally reversible and represents a new type of photochromic reaction of substituted anthraquinones.⁴ Unlike the photo-Fries rearrangement involving the homolytic cleavage of a carbon–heteroatom bond,² this photochemical migration is a concerted adiabatic process which proceeds on the triplet potential energy surface.^{4,5} An adiabatic mechanism of acyl migration was proposed based primarily on the analysis of energy correlation

SCHEME 1



diagrams and the dependence of the reactivity on the chemical structure.^{4b} This mechanism was later supported^{4c} by the recognition of 9-acetoxy-2-methoxy-1,10-anthraquinone in its triplet excited state ($^3\mathbf{2a}$), as the precursor of the ground state **2a**.

It should be noted that most well-studied photochemical reactions proceed nonadiabatically through conical intersections.⁶ Much less is known about adiabatic photochemical reactions, especially those proceeding on a triplet potential energy surface (PES).

A series of O-acylic derivatives of 1-hydroxy-2-methoxyanthraquinone with methyl (**1a**), ethoxyl (**1b**), and diethylamino (**1c**) groups in the migrating carbonyl moiety were studied using nanosecond laser flash photolysis.⁵ In all quinones under study (**1a–c**) the precursors of the *ana*-quinone products (**2a–c**) were detected and assigned to the triplet excited states of **2a–c** (Scheme 2). In the case of electron-donating substituents in the migrating carbonyl (**1b,c**) group, several short-lived intermediates were also detected and tentatively assigned to the triplet excited states of the *para*-quinones ($^3\mathbf{1b,c}^*$).⁵ However, the time

* Corresponding author. Telephone: 7(383) 333 3053. Fax: 7(383) 330 7350. E-mail: gritsan@kinetics.nsc.ru.

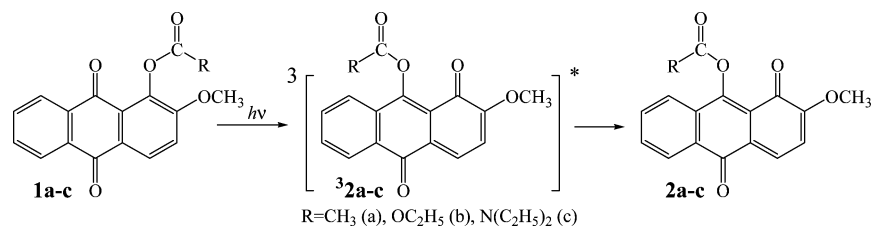
[†] The Ohio State University.

[‡] Institute of Chemical Kinetics and Combustion, Siberian Branch of Russian Academy of Sciences.

[§] Novosibirsk State University.

^{||} Adam Mickiewicz University.

SCHEME 2



resolution of the system (~ 3 ns) was not sufficient to detect $^3\mathbf{1a}^*$ nor to study the dynamics of the primary photophysical processes.

In this work we have applied ultrafast transient absorption spectroscopy to monitor the migration of acetoxy group on the triplet PES and the kinetics of the primary processes on the singlet PES. To support the assignment of the transient absorption spectra, the UV–vis spectra of the proposed intermediates were calculated using time-dependent density functional theory (DFT). In addition, a detailed analysis of the influence of the acyl group substitution on the rate constants of the photochemical and thermal migrations was performed using the results of the quantum chemical calculations.

Experimental and Computational Details

1-Acetoxy-2-methoxy-9,10-anthraquinone was synthesized following a published procedure.^{4a,c} Acetonitrile (Sigma-Aldrich, spectrophotometric grade) and squalane (2,6,10,15,19,23-hexamethyltetracosane, Sigma-Aldrich) were used as received.

Femtosecond Broad-Band UV–Vis Transient Absorption Experiments. Ultrafast experiments were performed in acetonitrile at room temperature. The absorbance of the sample solutions was about 0.7 (in a 1 mm cell) at an excitation wavelength of 270 nm. The transient absorption spectra were recorded on a femtosecond broad-band UV–vis transient absorption spectrometer.⁷ The laser system consists of a short pulse titanium–sapphire oscillator (Coherent, Mira) followed by a high-energy titanium–sapphire regenerative amplifier (Coherent, Positive Light, Legend HE USP). The main part of the beam is used to pump OPA (OPerA Coherent) equipped with a SFG module which generates a UV pump pulse tunable from 240 to 310 nm. A small part of the fundamental beam is focused into a 1 mm thick calcium fluoride plate to generate a white light continuum between 340 and 640 nm. The white light continuum is split into probe and reference beams of nearly equal intensity. The probe and reference beams pass through the sample, but only the probe beam overlaps with the pump beam in the sample. The pump pulse energy was about 6 μ J at the sample position. The sample is circulated in a Harrick Scientific flow cell (1 mm thick CaF₂ windows, optical path length 1 mm).

The detection system consists of an imaging polychromator (Triax 550 Jobin Yvon) and CCD camera (Symphony Jobin Yvon). Transient absorption spectra were registered at different pump–probe delay times using an optical delay line. To gauge the reproducibility of the data, the entire set of pump–probe delay positions was repeated at least three times.

The kinetic traces were analyzed by fitting to a sum of exponential terms. Convolution with a Gaussian response function was included in the fitting procedure. The instrument response was approximately 300 fs (fwhm).

Nanosecond Laser Flash Photolysis (LFP). An excimer XeCl laser (Lambda Physik, 308 nm, 20 ns, 50 mJ) was used as the excitation light source. The spectrometer has been described

previously.⁸ Solutions were prepared in spectroscopic-grade acetonitrile with an optical density (OD) of about 0.7 at 308 nm. Experiments were performed at ambient temperature (~ 295 K).

Quantum Chemical Calculations. The geometries of the ground singlet and lowest triplet states of 1-acyloxy-2-methoxy-9,10-anthraquinones (**1**) and 9-acyloxy-2-methoxy-1,10-anthraquinones (**2**) were calculated at the B3LYP^{9,10} level of theory with the 6-31G(d,p) basis set, using the Gaussian 03 suite of programs.¹¹ All equilibrium structures were ascertained to be minima on the potential energy surfaces, and the stability of the SCF solutions was tested. The values of the barriers of the photochemical and thermal acyl group migrations were evaluated at the same level of theory. The influence of the solvent on the energies of the stationary and transition points was taken into consideration by the PCM¹² models as implemented to Gaussian 03.

To predict the electronic absorption spectra, the time-dependent (TD) DFT method¹³ with the B3LYP combination of exchange⁹ and correlation functionals¹⁰ was used with the 6-31+G(d,p) basis set.

Results and Discussion

Transient Absorption Measurements. The sample solution of 1-acetoxy-2-methoxyanthraquinone (**1a**) in acetonitrile was pumped by a femtosecond laser pulse (270 nm). The calculations predict that **1a** has three transitions with large oscillator strength in the vicinity of 270 nm: at 285 ($S_0 \rightarrow S_7$, $f = 0.10$), 277 ($S_0 \rightarrow S_9$, $f = 0.19$), and 248 nm ($S_0 \rightarrow S_{11}$, $f = 0.23$). In the experimental absorption spectrum these transitions manifest themselves as a broad band with a maximum at 263 nm with shoulders at 251 and 282 nm (see Supporting Information, part 2, Figure 1S). Therefore, excitation at 270 nm results in the population of a set of highly excited singlet states. The long-wavelength-absorption band of **1a**, displayed as a dotted line in Figure 1a, belongs to the $S_0 \rightarrow S_2$ transition of the $\pi\pi^*$ type ($\lambda_{\max}(\text{exp}) = 362$ nm, $\lambda_{\max}(\text{calc}) = 387$ nm, $f = 0.07$). Calculations predict that the lowest singlet excited state of **1a** is the $^1n\pi^*$ state; transition to this state ($\lambda_{\max}(\text{calc}) = 423$ nm) has a very low intensity ($f = 0.002$) and is masked by the more intense $S_0 \rightarrow S_2$ band.

The transient absorption spectra produced by excitation of solutions of **1a** were recorded at different time delays between the probe and pump pulses. The transient absorption spectra, recorded over a 0–1 ns time window, are presented in Figures 1a–3a. Figure 1a depicts a broad transient absorption with a maximum at ~ 430 nm that is formed within the laser pulse. The transient absorption kinetics, shown in Figure 1b, were fitted to a sum of exponential terms with convolution using a Gaussian instrument response function included in the fitting procedure. The kinetics monitored at 404 nm were fitted with only one exponential term (130 ± 70 fs) since it is an isobestic point for further spectral transformations (Figure 2a). The kinetics at 580 nm were fitted to a sum of three exponential terms (for a detailed

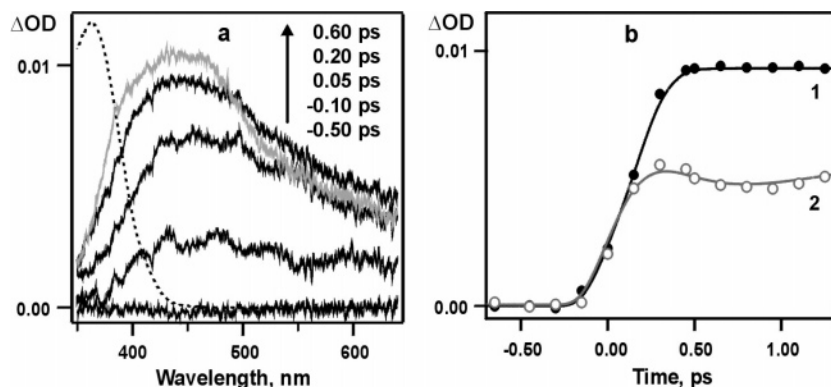


Figure 1. (a) Transient absorption spectra recorded over a -0.5 to 0.6 ps time window following fs pulsed photolysis of 1-acetoxy-2-methoxyanthraquinone (**1a**) in acetonitrile. The dotted line represents the $S_0 \rightarrow S_2$ absorption of **1a**. (b) Time dependence of the signals at 404 nm (1) and 580 nm (2). The solid lines represent the best fit by one (curve 1) and three (curve 2) exponential terms with a convolution using a Gaussian response function.

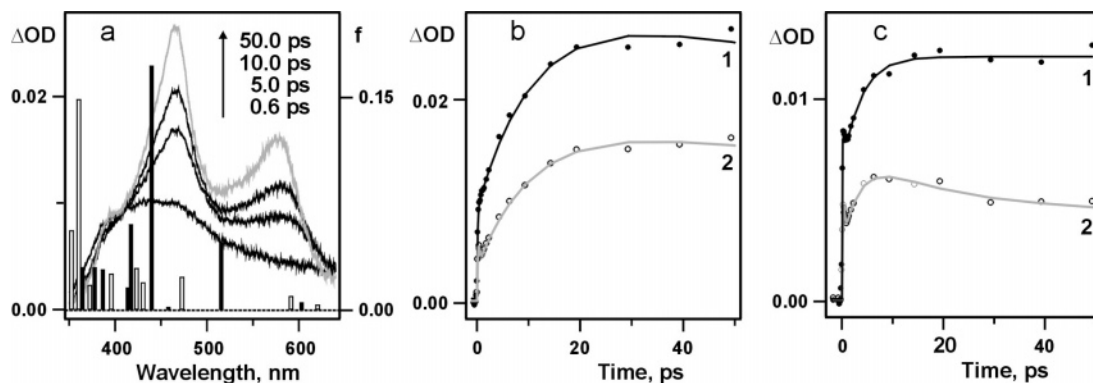


Figure 2. (a) Transient absorption spectra recorded over a 0.6 – 50 ps time window following fs pulsed photolysis of **1a** in acetonitrile. The vertical bars indicate the positions and oscillator strengths (f) of the electronic transitions calculated for **1a** in the triplet excited states of the $\pi\pi^*$ type (black bars) and $n\pi^*$ type (open bars). (b) Time dependence of the signals at 465 nm (1) and 580 nm (2). (c) Time dependence of the signals at 500 nm (1) and 620 nm (2). The solid lines represent the best fitting with a sum of three (b, curves 1 and 2; c, curve 1) and four (c, curve 2) exponential terms.

discussion, see below). The time constant of the primary process was found to be 150 ± 90 fs.

The population of highly excited singlet states is generally accompanied by ultrafast internal conversion to the lowest singlet excited state ($\tau \sim 100$ – 300 fs)¹⁴ and intramolecular vibrational energy redistribution (IVR, $\tau \sim 100$ – 200 fs).^{14c} Therefore, the transient absorption with a maximum at ~ 430 nm formed with a time constant of 150 ± 90 fs (Figure 1) is assigned to **1a** in the lowest singlet excited state (**1a**^{*}), presumably of the $^1n\pi^*$ type.

Figure 2a demonstrates that the decay of **1a**^{*} on the picosecond time scale is accompanied by the formation of a species with two absorption maxima at 465 and 580 nm. Similarly, two maxima in the range 400 – 650 nm were detected immediately after pulsed laser excitation (355 nm, 3 ns) of 1-acyloxy-2-methoxyanthraquinones with donor substituents in the migrating acyl group (**1b,c**, Scheme 2) and were assigned to their triplet–triplet (T–T) absorptions.⁵

Calculations predict that the two lowest excited triplet states ($^3n\pi^*$ and $^3\pi\pi^*$) of **1a** are very close in energy with the $^3n\pi^*$ state being slightly lower (1.5 kcal/mol) in the gas phase and higher (2.9 kcal/mol) in energy in acetonitrile (Supporting Information, part 1). Earlier^{4b} the dependence of the reactivity of **1** (Scheme 1) on the substitution in the quinone rings was explained by the conservation of orbital symmetry. Since only the $^3\pi\pi^*$ excited state can undergo acyl migration,^{4b,c} this state is likely to be the lowest excited states of compounds **1a–c**. Indeed the calculated T–T spectrum of $^3\pi\pi^*$ agrees much better

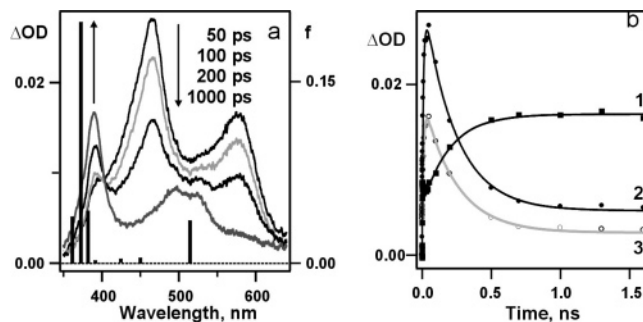


Figure 3. (a) Transient absorption spectra recorded over a 50 – 1000 ps time window. The vertical bars indicate the positions and oscillator strengths (f) of the electronic transitions calculated for **2a** in the triplet excited state. (b) Time dependence of the signals at 390 nm (1), 465 nm (2), and 580 nm (3). Solid lines represent the best fit with a sum of three exponential terms.

with experiment than that for $^3n\pi^*$ (Figure 2a). Although the two most intense transitions (440 and 515 nm) are noticeably blue-shifted from the experimental maxima (465 and 580 nm), agreement between the experiment and calculated spectra of $^3\pi\pi^*$ is quite good.

Therefore, on a time scale of tens of picoseconds we detected formation of the lowest $^3\pi\pi^*$ state of **1a** due to intersystem crossing from the excited singlet $n\pi^*$ state. The decay of $^3\pi\pi^*$ state (**3a**) is followed by the formation of a new species with absorption maxima at 390 , 500 , and 522 nm (Figure 3a). This spectrum was detected previously⁵ and assigned to the

TABLE 1: Extinction Coefficients at the Maximum of the $S_0 \rightarrow S_2$ Transition of **1a and the Estimated Values (Accuracy $\pm 10\text{--}15\%$) of the Extinction Coefficients for All of the Intermediates Detected in Acetonitrile**

compound/intermediate	1a	$^1\mathbf{1a}^*$	$^3\mathbf{1a}^*$	$^3\mathbf{2a}^*$	$\mathbf{2a}^{4c,5}$
λ_{\max} , nm	362	$\sim 375^a$	580, 465	500	510
ϵ , $M^{-1} \text{ cm}^{-1}$	6.3×10^3	$\sim 7.3 \times 10^3$	$7.2 \times 10^3, 1.2 \times 10^4$	3.6×10^3	1.1×10^4

^a Bleaching of **1a** was taken into account.

TABLE 2: Summary of the Kinetic Results for the Process of Thermally Reversible Adiabatic Photochemical Migration of Acetoxy Group in **1a in Acetonitrile (This Work) and Acyl Groups in **1a–c** in Toluene (Data of Ref 5)**

compd	solvent	k_{IC} , 10^{12} s^{-1}	k_{ISC} , 10^{10} s^{-1}	k_{VC} , 10^{11} s^{-1}	k_{photo} , 10^9 s^{-1}	k'_{ISC} , 10^5 s^{-1}	k''_{ISC} , 10^5 s^{-1}	k_{Therm} , 10^6 s^{-1}
1a	CH_3CN	7 ± 4	9.1 ± 0.8	2.5 ± 0.6	4.5 ± 0.6	8 ± 2		0.8 ± 0.2
1a ⁵	PhCH_3					8.8 ± 0.8		1.2 ± 0.1
1b ⁵	PhCH_3				8.2×10^{-2}	8.7 ± 0.8		6.5×10^{-3}
1c ⁵	PhCH_3				5.2×10^{-4}	1.4 ± 0.2	4.3 ± 0.4	2.9×10^{-6}

T–T absorption of the *ana*-quinone $^3\mathbf{2a}$ (Scheme 2). Indeed, the calculated spectrum of $^3\mathbf{2a}$ agrees perfectly with the transient spectrum detected nanoseconds after the laser pulse.

Note that the transient absorption spectra are displayed in Figures 1a–4a. However, for comparison with the calculations, one must estimate the contribution from bleaching of **1a** to the transient absorption spectra. This is possible if the extinction coefficients of **1a** and **2a** are known, and if one assumes that the photoexcitation of **1a** leads to **2a** with a quantum yield close to unity.⁵ Using the extinction coefficient of **2a** at 510 nm ($1.1 \times 10^4 \text{ M}^{-1} \text{ cm}^{-1}$),^{4c,5} we consecutively estimated the extinction coefficients of all of the proposed intermediates (Table 1). It is clear that the bleaching of **1a** is significant at $\lambda < 420$ nm and negligible at longer wavelengths (Figure 1a, Table 1).

The decay of the transient absorption of $^3\mathbf{2a}$ was detected on the nanosecond time scale (Figure 4) using the LFP apparatus. Its decay was accompanied by the formation of a final product **2a** (Figure 4a), which in turn reverts to **1a** on a microsecond time scale by thermal acetoxy group migration (Figure 4b). Figure 4a demonstrates that the spectrum of *ana*-quinone **2a** is very well reproduced by theory (again the bleaching of **1a** affects the UV portion of the transient absorption spectra). Note that the formation of persistent **2a** was previously discovered by photolysis of **1a** in glassy matrixes at 77 K.^{4a} Intersystem crossing of $^3\mathbf{2a}$ to the ground state and the dependence of its rate constant on the oxygen concentration as well as thermal acetoxy group migration have been studied in detail.^{4c,5}

Turning back to the femto- and picosecond time scale data, we consider more carefully the kinetics of the primary processes. Figures 2b and 3b represent the time dependence of the signals at the absorption maxima of $^3\mathbf{1a}$ (465 and 580 nm). These

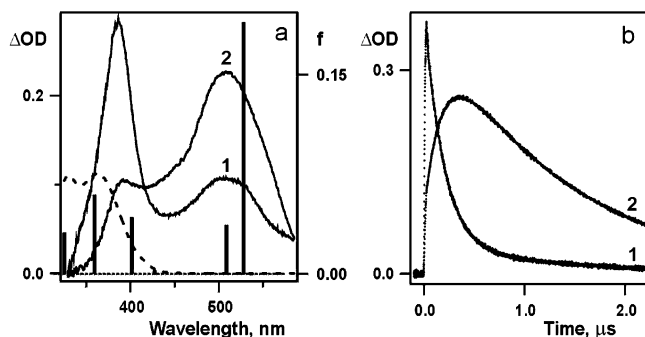
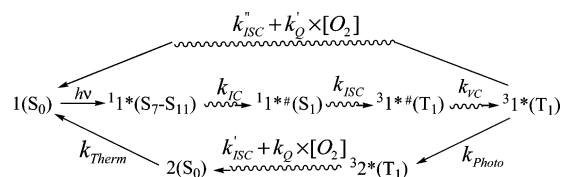


Figure 4. (a) Transient absorption spectra recorded 30 ns (1) and 270 ns (2) after the laser pulse (308 nm, 20 ns). The dotted line represents the spectrum of **1a** in the ground state. The vertical bars indicate the positions and oscillator strengths (f) of the electronic transitions calculated for **2a** in the ground state. (b) Time dependence of the signals at 390 nm (1) and 510 nm (2) in acetonitrile saturated by air and the best fitting by a sum of two exponential terms.

SCHEME 3



kinetics as well as the kinetics monitored at other wavelengths, except those recorded on the tails of the absorption bands, could be well fit to a sum of three exponential terms (taking into account a Gaussian response function).

The first exponential term with a time constant of 150 ± 90 fs was discussed above and is typical of an internal conversion and IVR process.¹⁴ The second exponential term has a time constant of 11 ± 1 ps and is assigned to intersystem crossing (ISC) from the $^1n\pi^*$ to the $^3\pi\pi^*$ state. The quantum yield of triplet formation is expected to be close to unity, which agrees with the quantum yield of **2a** formation (0.85 ± 0.17).⁵ The value of the ISC rate constant $\sim 10^{11} \text{ s}^{-1}$ is typical of intersystem crossing rates between states of different symmetries ($\pi\pi^*$ and $n\pi^*$).¹⁵

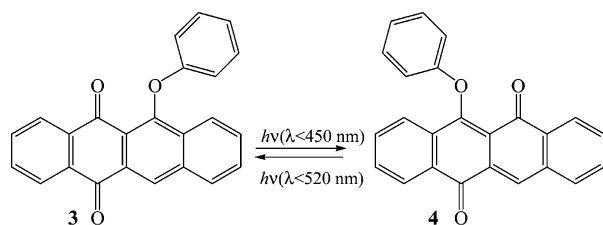
The final exponential term is assigned to the migration of the acetoxy group on the triplet potential energy surface and has a time constant of 220 ± 30 ps. Therefore, acetoxy group migration is significantly faster ($k = (4.5 \pm 0.6) \times 10^9 \text{ s}^{-1}$) than the migration of acyloxy groups with donor substituents (Scheme 2) with rate constants of $8.2 \times 10^7 \text{ s}^{-1}$ in **1b** ($R = \text{OC}_2\text{H}_5$) and $5.2 \times 10^5 \text{ s}^{-1}$ in **1c** ($R = \text{N}(\text{C}_2\text{H}_5)_2$).⁵

As mentioned above, the kinetics recorded at the red edges of the absorption bands of $^3\mathbf{1a}$ could not be satisfactorily fitted to a sum of three exponential terms; instead four exponential terms are needed to fit experimental kinetics on the picosecond time scale (Figure 2c). The fourth exponential term has a time constant of 4 ± 1 ps and relates to a slight narrowing of the $^3\pi\pi^*$ absorption bands (Figure 2a). This pattern is characteristic of vibrational cooling (VC) of species initially formed with excess vibrational energy.¹⁶ The 4 ps time constant is consistent with other reports of VC of polyatomic molecules.¹⁷

Therefore, the entire process of thermally reversible, adiabatic, photochemical migration of acyl groups in 1-acyloxy-2-methoxyanthraquinones (**1a–c**) can be described by Scheme 3, where $^1\mathbf{1}^{\#}$ and $^3\mathbf{1}^{\#}$ represent excited singlet and triplet *para*-quinones with excess vibrational energy. The rate constants of the elementary reactions are presented in Table 2.

The photochemical and thermal migrations of the more bulky acyl groups (**1b,c**) were studied previously in toluene, while all primary processes in **1a** were recorded in acetonitrile (Table 1), which is more convenient for studying femtochemistry. However, the rate constant of thermal acetoxy group migration

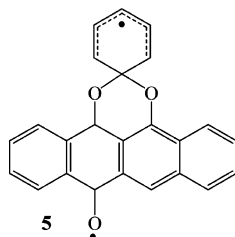
SCHEME 4



was found to be the same within experimental accuracy in toluene and acetonitrile (Table 2) as well as in ethanol.^{4c} We found that k_{Therm} depends on neither the polarity of the solvents nor its viscosity as the kinetics are the same in hexane and a very viscous solvent—squalane. It seems likely that the solvent has little influence on the rate constant of acyl group migration on the triplet PES.

A related photochemical migration of a bulky polyatomic group, viz., the phenyl group, has been reported for 6-phenoxy-5,12-anthraquinone (**3**, Scheme 4)¹⁸ as well as for substituted 1-phenoxyanthraquinones.^{4d}

In early studies^{18c,d} very similar transient absorption spectra were recorded upon LFP of **3** on the nanosecond time scale. However, this spectrum was attributed to different intermediates. Strokach et al.^{18c} assigned this spectrum to the spiro-bridged biradical intermediate **5** and proposed a nonadiabatic mechanism



of phenyl migration. On the other hand, Malkin et al.^{18d} attributed the same spectrum to a triplet excited state of *ana*-quinone **4** and concluded that photochemical phenyl group migration proceeds adiabatically on a triplet PES.

Recently,¹⁹ Wirz et al. carefully reinvestigated this system using subpicosecond pump–probe spectroscopy, nanosecond LFP, and photoacoustic and emission spectroscopies. Using these complementary techniques, the authors convincingly proved that the phototransformation of *para*-quinone **3** to *ana*-quinone **4** proceeds via a short-lived triplet state of **3** ($\tau \sim 2$ ns) and spiro-bridged biradical **5** ($\tau \sim 6$ ns). The long-lived triplet state of **4** detected upon nanosecond LFP^{18b,c} is formed by reexcitation of **4** and **5**, which are formed during the laser pulse.¹⁹ This explains why the long-lived transient absorption strongly depends on the intensity and duration of the laser pulse.¹⁹

In contrast to the case of **3**, the same transient absorption spectrum assigned to the triplet state of **2a** was detected upon femto- and nanosecond excitation of *para*-quinone **1a**, which excludes its formation by the reexcitation of **2a** or a spiro biradical similar to **5**. In addition, the quantum yield of **2a,b** formation is close to unity,⁵ as it should be in the case of a very fast adiabatic reaction on the triplet PES. On the contrary, the quantum yield of **4** is much less than unity (0.32)¹⁹ due to the decay of the biradical **5** to both isomers **3** and **4**.

Previously,²⁰ in order to choose between the proposed adiabatic and nonadiabatic mechanisms^{18b,c} of the quinone **3** phototransformation, we performed very simple AM1 calculations. We localized three minima on the triplet PES with the

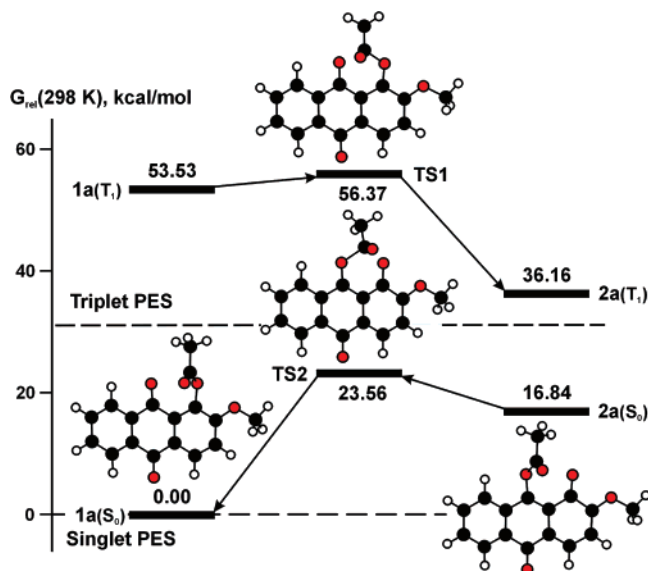


Figure 5. Relative free energies (in kcal/mol) of stationary points localized for photochemical and thermal migrations of the acetyl group in **1a** predicted by the B3LYP/6-31G(d,p) method and optimized structures of ³**1a**, ³**2a** and **1a**, **2a** and transition states for their interconversions (carbon atoms in black, oxygen atoms in red, hydrogen atoms as open circles) obtained at the same level.

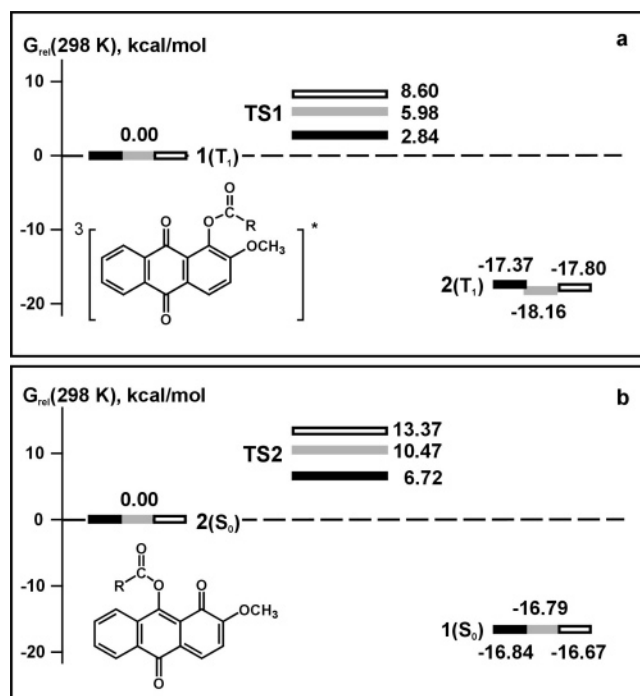


Figure 6. Influence of the acyl structure on relative free energies (in kcal/mol) of the stationary points for the photochemical (a) and thermal (b) migrations of the acyl ($-\text{C}(\text{O})\text{R}$) groups in the gas phase predicted by B3LYP/6-31G(d,p) calculations: black ($\text{R} = \text{CH}_3$), gray ($\text{R} = \text{OCH}_3$), and open ($\text{R} = \text{N}(\text{CH}_3)_2$) rectangles.

structures of ³**3**, ³**4**, and triplet biradical ³**5**. The deepest minimum on this PES corresponds just to the structure of ³**5**. This coincides with the experimental results of Wirz et al.¹⁹ confirming the nonadiabatic mechanism of quinone **3** photochemistry.

Therefore, different mechanisms, adiabatic and nonadiabatic, are realized in the photochemical migration of acyl and phenyl groups.

Quantum Chemical Calculations of the Ground State Singlet and Triplet Excited PESs. It was found previously⁵

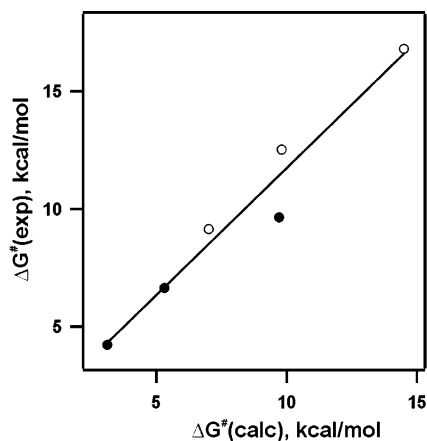


Figure 7. Correlation of experimental and calculated values of free energy of activation for the photochemical (black circles) and the thermal (open circles) acyl group migrations. The straight line is the best linear fit to the data ($R = 0.985$): $\Delta G^\ddagger(\text{exp}) = (0.3 \pm 0.9) + (1.2 \pm 0.1)\Delta G^\ddagger(\text{calc})$.

that acyl migrations on both the triplet and singlet ground state PESs are thermally activated with the activation energy increasing for the stronger donor substituents. We were able to localize all stationary points of acyl group migration on the triplet and singlet ground state PESs. Calculations were performed for the acyl groups (O–C(O)R), with R being CH₃, OCH₃, and N(CH₃)₂ similar to compounds **1a–c**. Note that a set of isomeric structures of *para*-quinones as well as *ana*-quinones was optimized. They differ from each other in terms of the orientations of methoxy and acetoxy substituents (all structures are presented in the Supporting Information, part 1). Transition state structures were localized only for the lowest energy isomers.

The stationary points localized for the acetyl group (C(O)–CH₃) migration (**1a**) are displayed in Figure 5 (PESs for migrations of C(O)CH₃ in acetonitrile and C(O)OCH₃ and C(O)N(CH₃)₂ in a vacuum and acetonitrile are given in the Supporting Information, part 2, Figures S2–S6). Figure 5 demonstrates that both migrations proceed through the transition states and the free energies (and enthalpies) of activation are significantly smaller for the migration in the triplet state. This agrees with the considerably larger (more than 3 orders of magnitude) rate constant of photochemical migration. The data presented in Figure 5 were calculated in the gas phase. However, calculations performed in the continuum field of acetonitrile using the PCM¹² model gave very similar results; the changes of the free energy of activation were within 10–15% (Supporting Information, part 2, Figure 7S). This agrees with our conclusion that the medium has little influence on the rate constant of acyl group migrations.

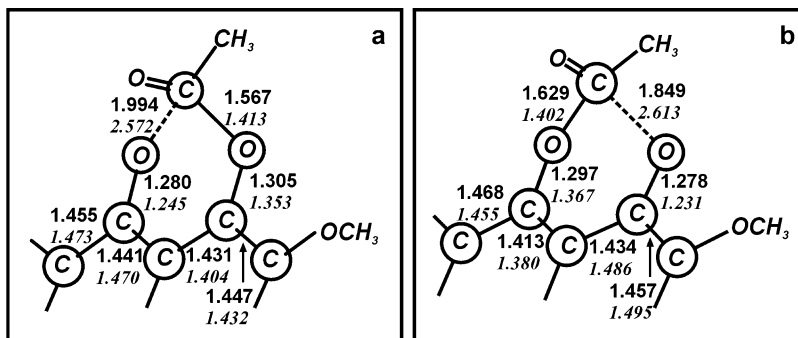


Figure 8. Selected bond lengths (in Å) of the reactive center for the acetoxy group migrations on the triplet (a) and singlet (b) PESs. The data in italics refer to the reactant structures (**31a** or **2a**, respectively) and the data in normal font refer to the transition states. All results were obtained at the (U)B3LYP/6-31G(d,p) level of theory.

Figure 6 demonstrates that substitution at the R position has only a very small influence on the free energy of migration (ΔG). In addition, very similar ΔG values were calculated for both the photochemical and the thermal acyl migrations. The influence of the acyl substitution on the free energy of activation (ΔG^\ddagger) is significant and is more pronounced for the photochemical process. To allow quantitative comparison with theory, we predicted the experimental values of ΔG^\ddagger according to the conventional formula

$$\Delta G^\ddagger(\text{exp}) = -RT \ln \left(\frac{k_{\text{exp}} h}{kT} \right)$$

The correlation of the experimental ΔG^\ddagger values with the calculated ones is displayed in Figure 7 and demonstrates excellent quantitative agreement between experiment and calculations at the B3LYP/6-31G(d,p) level of theory.

It is clear that the (U)B3LYP calculations adequately reproduce details of acyl group migrations on both the triplet and singlet PESs. For example, Figure 8 demonstrates the structures of the critical portion of the transition state for acetoxy group migrations in **1a**. It becomes evident on careful examination that changes in the bond lengths on going from the reactants to the transition states are noticeably larger for the ground state migration and this leads to the larger barrier and free energy of activation of the thermal reaction.

Conclusions

A comprehensive, quantitative mechanism of the physical and chemical processes which follow photoexcitation of 1-acetoxy-2-methoxyanthraquinones (**1a**) was established using femto- and nanosecond transient absorption spectroscopy. The most interesting feature of this photochemical reaction is the concerted, adiabatic rearrangement which proceeds on the triplet potential energy surface. The photochemical and thermally reversible transformations of 1-acyloxy-2-methoxyanthraquinones represent one of the few known photochromic reactions of substituted anthraquinones.^{4d}

Excitation of **1a** at 270 nm results in the population of a set of highly excited singlet states. Internal conversion to the lowest singlet $n\pi^*$ excited state and IVR proceed with a time constant of 150 ± 90 fs. The $^1n\pi^*$ excited state undergoes very fast intersystem crossing (11 ± 1 ps) to the lowest triplet $\pi\pi^*$ excited state, which is formed with excess vibrational energy. Vibrational cooling occurs with a time constant of 4 ± 1 ps. The primary photochemical process, migration of the acetoxy group, proceeds on the triplet potential energy surface with a time constant of 220 ± 30 ps.

All assignments of the transient absorption spectra reported in this work were supported by quantum chemical calculations. In addition, all of the stationary points for acyl group ($-C(O)R$) migration on the triplet and singlet potential energy surfaces were located. The influence of substitution at the R position on the rate constants of the photochemical and thermal processes was analyzed.

Acknowledgment. Ultrafast studies were performed at the Ohio State University Center for Chemical and Biophysical Dynamics. Support of this work, and of the CCBP, by the National Science Foundation and by the Ohio Supercomputer Center is gratefully acknowledged.

Supporting Information Available: Cartesian coordinates of all stationary points located in this study (part 1); details of the time-dependent density functional calculations of the electronic absorption spectra and relative free energies of the stationary points on the singlet and triplet PESs (part 2). This material is available free of charge via the Internet at <http://pubs.acs.org>.

References and Notes

- (1) (a) Fries, K.; Finch, G. *Ber. Deutsch. Chem. Ges.* **1908**, *41*, 4271. (b) Martin, R. *Org. Prep. Proced. Int.* **1992**, *24*, 369. (c) Traven, V. F. *Molecules* **2004**, *9*, 50.
- (2) (a) Anderson, J. C.; Reese, C. B. *Proc. Chem. Soc., London* **1960**, 217. (b) Bellus, D. *Adv. Photochem.* **1971**, *8*, 109. (c) Meyer, J. W.; Hammond, G. S. *J. Am. Chem. Soc.* **1972**, *94*, 2219. (d) Kalmus, C. E.; Hercules, D. S. *J. Am. Chem. Soc.* **1974**, *96*, 449. (e) Gritsan, N. P.; Tsentalovich, Yu. P.; Yurkovskaya, A. V.; Sagdeev, R. Z. *J. Phys. Chem.* **1996**, *100*, 4448. (f) Gu, W.; Weiss, R. G. *J. Photochem. Photobiol., C: Photochem. Rev.* **2001**, *2*, 117.
- (3) Kaanumalle, L. S.; Gibb, C. L. D.; Gibb, B. C.; Ramamurthy, V. *Org. Biomol. Chem.* **2007**, *5*, 236.
- (4) (a) Gritsan, N. P.; Russkikh, S. A.; Klimenko, L. S.; Fokin, E. P. *Teor. Eksp. Khim.* **1983**, *19*, 455. (b) Gritsan, N. P. *J. Mol. Struct. (THEOCHEM)* **1988**, *181*, 285. (c) Gritsan, N. P.; Klimenko, L. S.; Shvartsberg, E. M.; Khmelinski, I. V.; Fokin, E. P. *J. Photochem. Photobiol., A: Chem.* **1990**, *52*, 137. (d) Gritsan, N. P.; Klimenko, L. S. *Photochem. Photobiol., A: Chem.* **1993**, *70*, 103.
- (5) Gritsan, N. P.; Kellmann, A.; Tfibel, F.; Klimenko, L. S. *J. Phys. Chem. A* **1997**, *101*, 794.
- (6) (a) Zimmerman, H. E. *J. Am. Chem. Soc.* **1966**, *88*, 1566. (b) Michl, J. *J. Mol. Photochem.* **1972**, 243. (c) Bernardi, F.; Olivucci, M.; Robb, M. A. *Chem. Soc. Rev.* **1996**, *25*, 321.
- (7) Burdzinski, G.; Hackett, J. C.; Wang, J.; Gustafson, T. L.; Hadad, C. M.; Platz, M. S. *J. Am. Chem. Soc.* **2006**, *128*, 13402.
- (8) Tsao, M.-L.; Gritsan, N. P.; James, T. R.; Platz, M. S.; Hrovat, D.; Borden, W. T. *J. Am. Chem. Soc.* **2003**, *125*, 9343.
- (9) Becke, A. D. *J. Chem. Phys.* **1993**, *98*, 5648.
- (10) Lee, C.; Yang, W.; Parr, R. G. *Phys. Rev. B* **1988**, *37*, 785.
- (11) Frisch, M. J.; et al. *Gaussian 03*, revision C.02; Gaussian, Inc.: Wallingford, CT, 2004 (full reference given in Supporting Information).
- (12) (a) Miertus, S.; Scrocco, E.; Tomasi, J. *Chem. Phys.* **1981**, *55*, 117. (b) Cossi, M.; Barone, V.; Cammi, R.; Tomasi, J. *Chem. Phys. Lett.* **1996**, *255*, 327. (c) Tomasi, J.; Mennucci, B.; Cammi, R. *Chem. Rev.* **2005**, *105*, 2999.
- (13) (a) Dreuw, A.; Head-Gordon, M. *Chem. Rev.* **2005**, *105*, 4009. (b) Casida, M. E.; Jamorski, C. K.; Casida, C.; Salahub, D. R. *J. Chem. Phys.* **1998**, *108*, 4439. (c) Wiberg, K. B.; Stratmann, R. E.; Frisch, M. J. *Chem. Phys. Lett.* **1998**, *297*, 60.
- (14) (a) Ohta, K.; Kang, T. J.; Tominaga, K.; Yoshihara, K. *Chem. Phys.* **1999**, *242*, 103. (b) Billsten, H. H.; Zigmantas, D.; Sundstrom, V.; Polivka, T. *Chem. Phys. Lett.* **2002**, *355*, 465. (c) Baskin, J. S.; Yu, H.-Z.; Zewail, A. H. *J. Phys. Chem. A* **2002**, *106*, 9837.
- (15) Plotnikov, V. G.; Ovchinnikov, A. A. *Russ. Chem. Rev. (Usp. Khim.)* **1978**, *47*, 444. (b) Burdzinski, G.; Ziolk, M.; Karolczak, J.; Maciejewski, A. *J. Phys. Chem. A* **2004**, *108*, 11160.
- (16) (a) Laermar, F.; Elsaesser, T.; Kaiser, W. *Chem. Phys. Lett.* **1989**, *156*, 38. (b) Miyasaka, H.; Hagihira, M.; Okada, T.; Mataga, N. *Chem. Phys. Lett.* **1992**, *188*, 259. (c) Schwarzer, D.; Troe, J.; Votsmeier, M.; Zerezke, M. *J. Chem. Phys.* **1996**, *105*, 3121.
- (17) (a) Wong, V.; Gruebele, M. *J. Phys. Chem. A* **1999**, *103*, 10664. (b) Kovalenko, S. A.; Schanz, R.; Hennig, H.; Ernsting, N. P. *J. Chem. Phys.* **2001**, *115*, 3256. (c) Gruebele, M. *Adv. Chem. Phys.* **2001**, *114*, 193. (d) Burdzinski, G.; Maciejewski, A.; Buntinx, G.; Poizat, O.; Lefumeux, C. *Chem. Phys. Lett.* **2003**, *368*, 745.
- (18) (a) Gerasimenko, Yu. E.; Poteleschenko, N. T. *Zh. Org. Khim.* **1971**, *7*, 2413. (b) Strokach, Yu. P.; Barachevskii, V. A.; Sokoluk, N. T.; Gerasimenko, Yu. E. *Khim. Fiz.* **1987**, *6*, 320. (c) Malkin, J.; Zelichenok, A.; Krongauz, V.; Dvornikov, A. S.; Rentzepis, P. M. *J. Am. Chem. Soc.* **1994**, *116*, 1101.
- (19) Born, R.; Fischer, W.; Heger, D.; Tokarczyk, B.; Wirz, J. *Photochem. Photobiol. Sci.* **2007**, *6*, 552.
- (20) Gritsan, N. *Mol. Cryst. Liq. Cryst.* **1997**, *297*, 167.